Theor Chem Acc (1998) 99:231–240
DOI 10.1007/s0021498000m4

Theoretical
Chemistry Accounts

Regular article

Quantum Monte Carlo study of Be_2 and group 12 dimers M_2 (M = Zn, Cd, Hg)

F. Schautz, H.-J. Flad, M. Dolg

Max-Planck-Institut für Physik komplexer Systeme, Nöthnitzer Strasse 38, D-01187 Dresden, Germany

Received: 8 January 1998 / Accepted: 5 March 1998 / Published online: 13 July 1998

Abstract. Pure diffusion quantum Monte Carlo calculations have been carried out for Be_2 and the weakly bound group 12 dimers Zn_2, Cd_2 and Hg_2. We have applied relativistic energy-consistent large-core pseudopotentials and corresponding core-polarization potentials for the group 12 atoms. The derived spectroscopic constants (R_e, D_e, ω_e for Zn_2 and Cd_2 (Zn_2: 3.88 ± 0.05 Å, 0.024 ± 0.007 eV, 25 ± 2 cm^{-1}; Cd_2: 4.05 ± 0.03 Å, 0.031 ± 0.005 eV, 21 ± 1 cm^{-1}) are in good agreement with corresponding coupled-cluster results (Zn_2: 4.11 Å, 0.022 eV, 21 cm^{-1}; Cd_2: 4.23 Å, 0.029 eV, 18 cm^{-1}) and available experimental data (Zn_2: 0.034 eV, 26 cm^{-1}; Cd_2: 0.039 eV, 23 cm^{-1}). A comparison with previous results for the heavier homologue Hg_2 is made. Using a multi-reference trial wavefunction for Be_2 we achieved a sufficiently accurate description of the nodes of the wavefunction to obtain a bonding interaction within the fixed-node approximation. The applicability of this approach has been justified in pseudopotential and all-electron calculations. Covalent bonding contributions which appear in addition to pure van der Waals interactions for these molecules are analysed in terms of local occupation number operators and the associated interatomic charge fluctuations. Static dipole polarizabilities for group 12 atoms and dimers are calculated using a differential quantum Monte Carlo method for finite external electric fields. We have extended this method to pseudopotential calculations by taking into account the electric field dependence of the localized pseudopotentials. Within the statistical uncertainties our results agree with those from coupled-cluster calculations.

Key words: Quantum Monte Carlo – Relativistic pseudopotentials – Static dipole polarizabilities – van der Waals molecules – Fixed-node approximation

Correspondence to: H.-J. Flad

1. Introduction

The dimers of the group 12 atoms Zn, Cd and Hg have only a very weakly bound $^1\sum_g^+(0_g^+)$ ground state, but several well-bound excited states and were considered as possible candidates for excimer laser substances. Therefore, these systems have been frequently studied in the past both by experimentalists [1–5] and theoreticians [6–15]. The weak bonding interaction in the ground state is usually denoted as a van der Waals or dispersion interaction. Highly correlated wavefunctions including at least scalar-relativistic effects are needed to get reliable answers for the spectroscopic constants [7, 10, 11, 15]. Size-extensive standard correlation approaches like coupled-cluster methods together with quite large one-particle basis sets and relativistic pseudopotentials yield satisfactory results after correction of the basis set superposition error [15].

In the present contribution, we want to explore the quantum Monte Carlo (QMC) method as an alternative correlation treatment. It is not our intention to surpass the previously achieved results [15], instead the present work has been done in preparation of QMC studies for small and medium-sized clusters of Zn and Cd atoms. It has recently been shown that QMC is a useful approach for the study of medium-sized Hg clusters [16]. An interesting feature of Cd, Zn, and Hg clusters is the change of bonding with increasing cluster size from van der Waals interaction through covalent to metallic types of bonding occuring already at a relatively small number of atoms. QMC seems to be well-suited to study size-dependent properties since the method scales quite favourably with cluster size. For small clusters the bonding is mainly of the van der Waals type. Recent QMC studies of the van der Waals dimer He_2 by Anderson et al. [17] yielded a very accurate potential curve, and proved that QMC techniques can also be applied to very weakly interacting systems despite the inherent statistical uncertainties in any practical QMC calculation. In the case of the group 12 dimers two problems occur. First, the number of electrons to be considered is at least an order of

magnitude larger ($Zn_2 = 60$, $Cd_2 = 96$, $Hg_2 = 160$) and the shells giving the main bonding contributions are of different main quantum number [(n−1)d and ns, n = 4, 5, 6 for Zn, Cd, Hg]. Second, relativistic effects will contribute and cannot be entirely neglected for accurate work, e.g. at least a scalar-relativistic scheme is needed. Relativistic energy-consistent large-core pseudopotentials (PP) treating Zn, Cd, and Hg as two-valence-electron atoms together with the corresponding core-polarization potentials (PP) reduce the computational effort roughly to that needed for He_2, and also allow inclusion of implicitly scalar-relativistic effects by means of parametrization. The goal of the present paper is to show that the combination of pseudopotentials for relativistic effects and QMC for correlation effects accurately describes the weak bonding in the heavy- element systems Zn_2 and Cd_2 with the same accuracy as previously obtained for Hg_2[11]. Furthermore, we want to demonstrate the feasibility of QMC calculations for static dipole polarizabilities since they contribute to the leading order in van der Waals type interactions.

Bonding in Hg_2 has been recently analysed by Kunz et al. [12]. According to their findings Hg_2 should be thought of as an intermediate between a pure van der Waals complex and a chemically bound system. Using a different approach [18] to analyse large-scale multiconfiguration self-consistent field (MCSCF) wavefunctions Yu and Dolg [15] came to the same conclusion and found a similar bonding situation for Zn_2, Cd_2 and Hg_2. The latter analysis was based on interatomic charge fluctuations which were determined in a basis of localized atomic orbitals. In the present contribution a similar strategy is followed, however, the partitioning of the wavefunction into atomic subspaces is not achieved by means of localized orbitals but by a local operator defined in position space. The charge fluctuations are calculated using QMC for the "exact" wavefunctions and compared to the corresponding Hartree-Fock (HF) results.

For comparison it is also interesting to consider the Be_2 molecule which possesses the same valence electron configuration and is well-known for the strong covalent contributions to the bonding connected with near-degeneracies [19]. The charge fluctuations for this molecule are compared with those of Zn_2, Cd_2, and Hg_2. The calculations are complicated by the fact that it is necessary to use a multi-reference trial wavefunction which takes into account all the configurations contributing to the near-degeneracies.

2. Theory

2.1. Pseudopotentials and valence basis sets

Quasirelativistic energy-consistent ab initio pseudopotentials have been used to replace 28, 46 and 78 core-electrons for Zn, Cd and Hg, respectively, i.e. only the n*s* shell (n = 4, 5, 6 for Zn, Cd and Hg) is treated explicitly for the atomic ground states. The scalar-relativistic molecular valence model Hamiltonian in atomic units,

$$H = -\frac{1}{2}\sum_i \Delta_i + \sum_i V_{pp}(i) + \sum_{i<j}\frac{1}{r_{ij}} + \sum_{\nu<\mu}\frac{Q_\nu Q_\mu}{r_{\nu\mu}} + V_{CPP} \quad , \tag{1}$$

contains for each electron i a molecular pseudopotential $V_{pp}(i)$, which is assumed to be a superposition of semilocal atomic terms

$$V_{pp}(i) = \sum_\nu \left(-\frac{Q_\nu}{r_{i\nu}} + \sum_l V_{\nu,l}(r_{i\nu}) P_l(\vec{r}_{i\nu}/r_{i\nu}) \right). \tag{2}$$

i and j are electron indices, ν and μ are core indices. Q_ν denotes the charge of the core ν. l is the angular quantum number and $P_{\nu,l}$ denotes the projection operator on the angular symmetry l with respect to core ν. In the energy-consistent pseudopotential method the free parameters in the radial pseudopotential $V_{\nu,l}$ are adjusted to reproduce total valence energies derived from all-electron calculations for a multitude of many-electron states. The semiempirical core-polarization potential V_{CPP} accounts for static and dynamic core-polarization, i.e. non-frozen-core effects at the uncorrelated level and core-valence correlation effects at the correlated level. We adopt a form originally introduced by Müller et al. [20] and previously applied by Fuentealba et al. [21] to pseudopotential calculations:

$$V_{CPP} = -\frac{1}{2}\sum_\nu \alpha_\nu \vec{f}_\nu^{\,2} \tag{3}$$

with the electric field $\vec{f}_\nu$ at core ν multiplied by a cut-off function

$$\vec{f}_\nu = -\sum_i \frac{\vec{r}_{i\nu}}{r_{i\nu}^3}(1-\exp(-\delta^\nu r_{i\nu}^2)) + \sum_{\mu\neq\nu} Q_\mu \frac{\vec{r}_{\mu\nu}}{r_{\mu\nu}^3}(1-\exp(-\delta^\nu r_{\mu\nu}^2)) \quad . \tag{4}$$

The Hg pseudopotential and core-polarization potential have been taken from previous work [22]. The corresponding parameters for Zn and Cd are listed in Table 1. Even-tempered diffuse basis functions were added to optimized (4*s*4*p*) valence basis sets. For coupled-cluster calculations the basis sets were further extended by polarization functions. A single exponent for d, f and g type basis functions was optimized in atomic configuration interaction calculations. From these exponents we generated the polarization basis sets again in an even-tempered manner. The final uncontracted (7*s*7*p*5*d*3*f*1*g*) and (6*s*6*p*5*d*3*f*1*g*) valence basis sets for Zn and Cd, respectively, are listed in Table 2.

2.2. Correlation treatment

In order to obtain reference data for comparison with the QMC results we performed large-scale coupled-cluster calculations including single and double excitation operators as well as triple excitations by perturbation theory (CCSD(T)), similar to those reported

Table 1. Parameters of the relativistic large-core (Q = 2) pseudopotentials and core-polarization potentials for Zn, Cd and Hg

	Zn		Cd		Hg	
	a_{lk}	A_{lk}	a_{lk}	A_{lk}	a_{lk}	A_{lk}
s	1.498802	18.316720	1.4399372	15.5730800	10.000248	48.780475
	0.749005	−3.405011	0.2322784	−0.3737086	1.657530	27.758105
					0.227210	−0.696178
p	1.532770	11.464304	1.4594146	10.3781361	0.647307	8.575637
	0.787091	−1.327391	0.9706640	−0.0041229	0.398377	−2.735811
d	0.750276	1.583946	0.3748675	1.6664640	0.386058	2.792862
	0.374792	0.333476	0.6533233	−0.1895933	0.217999	−0.013118
f	0.466699	−0.398428	0.9762389	−11.2057425	0.500000	−2.635164
δ, α	0.3893	2.296	0.3032	4.971	0.2380	7.377

Table 2. Valence basis sets for Zn, Cd and Hg

	Zn	Cd	Hg
s	1.572755	1.599911	1.354842
	1.198905	0.742260	0.828892
	0.148856	0.116465	0.133932
	0.051016	0.042854	0.051017
	0.020406	0.014285	0.017
	0.008163	0.004762	0.006
	0.003265		
p	1.090807	0.888189	1.000146
	0.215688	0.166089	0.866453
	0.072211	0.059624	0.118206
	0.023185	0.020334	0.035155
	0.009274	0.006778	0.012
	0.003710	0.002259	0.004
	0.001484		
d	1.375	1.1875	1.188
	0.55	0.475	0.475
	0.22	0.19	0.19
	0.088	0.076	0.076
	0.0352	0.0304	0.0304
f	0.75	0.725	0.625
	0.30	0.29	0.25
	0.12	0.116	0.1
g	0.38	0.33	0.28

previously for Hg_2 [10]. These calculations were carried out with the MOLPRO program system [23]. Pure diffusion Monte Carlo (PDMC) has been applied as described in detail in our previous work on Hg_2 [11].

2.3. Dipole polarizabilities

The dispersion interaction in weakly bound van der Waals molecules can be expressed in terms of the static and dynamic dipole polarizabilities of their constituents [24]. Calculation of dynamic polarizabilities within the QMC method, is faced with conceptual difficulties and has been performed for two-electron systems only [25–27], so far.

Static dipole polarizabilities α_D can be calculated in QMC either by the differential QMC method proposed by Wells [28] or by the infinitesimal differential diffusion QMC method of Vrbik et al. [29]. In the first approach small finite fields are applied to the system and the total energies are determined from a correlated random walk which enables an accurate calculation of energy differences. This approach has been applied by Huiszoon and Briels [30] for the calculation of the static dipole polarizabilities of He and H_2. Although energy differences can be obtained with a much higher absolute accuracy than total energies, its application to polarizabilities requires second derivatives which are numerically more demanding. In order to avoid these difficulties Vrbik et al. [29] performed the differentiation of the energy expectation value with respect to an external field analytically, and sampled the resulting cumulant like expression of the dipole moment using an almost accurate sampling algorithm for the exact electron distribution [31, 32]. Within their formalism it is also possible to calculate hyperpolarizabilities with reasonably small statistical errors, e.g. their results for LiH are in good agreement with those of other ab initio calculations.

So far these methods have only been applied in all-electron calculations. Pseudopotentials introduce a slight difficulty in this approach, since they depend in its localized form implicitly on the external field due to the response of the localization function on the external field. The second derivative $\partial_\lambda^2 E(\lambda)|_{\lambda=0}$ of the energy expectation value for the exact field-dependent ground-state wavefunction $\boldsymbol{\psi}(\lambda)$ with respect to the field strength λ of an external homogeneous electrostatic field depends only on the first derivative $\partial_\lambda \boldsymbol{\psi}(\lambda)|_{\lambda=0}$ taking advantage of the Hellmann-Feynman theorem. In QMC $\boldsymbol{\psi}(\lambda)$ is generated from a trial wavefunction $\Phi(\lambda)$ by

$$\Psi(\lambda) = \lim_{\tau\to\infty} N(\tau)\exp[-(\hat{H}_0 + \hat{V}_\lambda)\tau]\Phi(\lambda) \ , \qquad (5)$$

where $\hat{V}_\lambda$ includes all the field-dependent parts in the Hamiltonian and $N(\tau)$ represents a τ dependent normalization constant. For correlated random walks it is convenient to replace $\Phi(\lambda)$ in Eq. (5) by $\Phi(0)$, which permits performance of a random walk independent of the field strength [28]. In our first application to the atoms Zn, Cd and Hg where we have a two-electron ground-state wavefunction without nodes, it is possible to omit the field dependence of the trial wavefunction Φ without any loss of accuracy. In the more general case of Zn_2, Cd_2 and Hg_2 where the trial wavefunction is used to specify the nodes the situation is somewhat different. Neglecting the response of the nodes on the external field imposes an additional approximation whose implications have not been studied so far systematically. We only want to mention that the results of Vrbik et al. [29]

for LiH are based on this approximation and yield good agreement with experimental values and other ab initio methods. Altogether, we obtain an expression for $\partial_\lambda^2 E(\lambda)|_{\lambda=0}$ which depends on the first and second derivative $(\partial_\lambda \hat{V}_\lambda|_{\lambda=0}, \partial_\lambda^2 \hat{V}_\lambda|_{\lambda=0})$ of the field-dependent potential $\hat{V}_\lambda$ only. In order to take this into account we have performed a Taylor expansion of the localized pseudopotential in terms of the external field:

$$\frac{V_{pp}\Phi(\lambda)}{\Phi(\lambda)} \approx \frac{V_{pp}\Phi(0)}{\Phi(0)} + \partial_\lambda \frac{V_{pp}\Phi(\lambda)}{\Phi(\lambda)}\Big|_{\lambda=0}\lambda + \frac{1}{2}\partial_\lambda^2 \frac{V_{pp}\Phi(\lambda)}{\Phi(\lambda)}\Big|_{\lambda=0}\lambda^2 \dots \quad . \tag{6}$$

Since we are not interested in the total values for $E(\lambda)$ but only in its second derivative $\partial_\lambda^2 E(\lambda)\big|_{\lambda=0}$ it is not necessary to go beyond second order in the expansion. Higher-order terms which affect $E(\lambda)$ will cancel for the derivative.

In QMC a spin-free formalism is employed where the spatial wavefunction is given by a product $\Phi = F|\Phi_\alpha||\Phi_\beta|$ with correlation factor F and Slater determinants $|\Phi_\alpha|$ and $|\Phi_\beta|$, which provide the correct permutational symmetry for fermions, see e.g. Ref. [33]. Since V_{pp} is a one-body operator the localized pseudopotential (Eq. 6) can be split up into two equivalent parts which act on $|\Phi_\alpha|$ and $|\Phi_\beta|$ separately. In the following, we will suppress α and β and assume that all the indices are running over the corresponding subset only. The inverse of a Slater matrix (first index refers to the electron, second index to the orbital) which belongs to a Slater determinant $|\Phi|$ is denoted by $|\Phi|^{-1}$.

The left-hand side of Eq. (6) can be brought into a form suitable for computation [34, 35]

$$\sum_{i,k,l} V_l(r_i) Z_{l0}(0,0) \int d\Omega_i' Z_{l0}(\varphi_i', \theta_i') \times \frac{F(\dots, \vec{r}_i', \dots)}{F(\dots, \vec{r}_i, \dots)} \phi_k(\vec{r}_i') \Phi_{ik}^{-1}(\dots, \vec{r}_i, \dots) \quad , \tag{7}$$

where Z_{lm} denotes real spherical harmonics. The two-dimensional angular integral has to be done numerically. From this expression it is straightforward to obtain the first

$$\sum_{i,k,l} V_l(r_i) Z_{l0}(0,0) \int d\Omega_i' Z_{l0}(\varphi_i', \theta_i') \frac{F(\dots, \vec{r}_i', \dots)}{F(\dots, \vec{r}_i, \dots)} \times [\partial_\lambda \phi_k(\vec{r}_i') \Phi_{ik}^{-1}(\dots, \vec{r}_i, \dots) + \phi_k(\vec{r}_i') \partial_\lambda \Phi_{ik}^{-1}(\dots, \vec{r}_i, \dots)] \tag{8}$$

and second

$$\sum_{i,k,l} V_l(r_i) Z_{l0}(0,0) \int d\Omega_i' Z_{l0}(\varphi_i', \theta_i') \frac{F(\dots, \vec{r}_i', \dots)}{F(\dots, \vec{r}_i, \dots)} \times [\partial_\lambda^2 \phi_k(\vec{r}_i') \Phi_{ik}^{-1}(\dots, \vec{r}_i, \dots) + \phi_k(\vec{r}_i')\, \partial_\lambda^2 \Phi_{ik}^{-1}(\dots, \vec{r}_i, \dots) + 2\partial_\lambda \phi_k(\vec{r}_i') \partial_\lambda \Phi_{ik}^{-1}(\dots, \vec{r}_i, \dots)] \tag{9}$$

derivative with respect to an external electric field. We have assumed that the correlation factor F does not depend on the electric field. The derivatives $\partial_\lambda \phi_k$ and $\partial_\lambda^2 \phi_k$ of the orbitals can be expressed in terms of the derivatives of the orbital coefficients in the basis set. This makes the calculation of the higher-order terms straightforward since the derivatives of the coefficients can be calculated in advance by numerical differentiation using orbital coefficients from finite- field HF calculations. The first and second derivatives of the inverse Slater matrix Φ^{-1} and Slater determinant $|\Phi|$ do not require any further field-dependent components:

$$\partial_\lambda \Phi_{ij}^{-1} = -\Phi_{ik}^{-1} \partial_\lambda \phi_l(k) \Phi_{lj}^{-1} \quad , \tag{10}$$

$$\partial_\lambda |\Phi| = \Phi_{ik}^{-1} \partial_\lambda \phi_i(k) |\Phi| \quad , \tag{11}$$

$$\partial_\lambda^2 \Phi_{ij}^{-1} = -\partial_\lambda \Phi_{ik}^{-1} \partial_\lambda \phi_l(k) \Phi_{lj}^{-1} - \Phi_{ik}^{-1} \partial_\lambda \phi_l(k) \partial_\lambda \Phi_{lj}^{-1} - \Phi_{ik}^{-1} \partial_\lambda^2 \phi_l(k) \Phi_{lj}^{-1} \quad , \tag{12}$$

$$\partial_\lambda^2 |\Phi| = \left[\Phi_{ik}^{-1} \partial_\lambda^2 \phi_i(k) + \partial_\lambda \Phi_{ik}^{-1} \partial_\lambda \phi_i(k) + \left(\frac{\partial_\lambda |\Phi|}{|\Phi|} \right)^2 \right] |\Phi| \quad . \tag{13}$$

Here we have assumed Einstein's summation convention for indices occuring twice. Equation (10) can be immediately obtained from the definition of the inverse Slater matrix

$$\delta_{ij} = \Phi_{ik}^{-1} \phi_j(k) \tag{14}$$

by differentiation with respect to the external electric field. The derivative of the Slater determinant (Eq. 11) can be obtained similarly to the derivatives for the cartesian coordinates (see e.g. [36]). From these equations the second derivatives can be obtained in a straightforward manner.

The Taylor expansion of the localized pseudopotential with respect to the external electric field strength λ introduces possibly singular terms of the general form $\partial_\lambda^n \Phi/\Phi$ at the nodes of the trial wavefunction Φ. An exception are two-electron systems as in our treatment of Zn, Cd and Hg, where Φ has no nodes. The degree of these singularities is important for applications of this method to larger systems. In our calculations we have assumed fixed nodes which do not depend on λ. In this case it seems plausible to suppose that the ratio between trial wavefunctions at finite field $\Phi(\lambda)$ and at zero field $\Phi(0)$ also remains finite close to the nodes. If we further suppose that a Taylor expansion of this ratio

$$\frac{\Phi(\lambda)}{\Phi(0)} = \sum_{n=0} \frac{\partial_\lambda^n \Phi(\lambda)}{\Phi(0)}\Big|_{\lambda=0} \frac{\lambda^n}{n!} \tag{15}$$

can be performed which remains valid close to the nodes of the trial wavefunction, the ratios $\partial_\lambda^n \Phi/\Phi$ are required not to diverge near the nodes. Therefore, the higher order terms in Eq. (6) are not more singular than the zeroth-order term. Unfortunately this is not exactly true in practical calculations. We have already mentioned above that the derivatives of the orbitals with respect to the external electric field are obtained from conventional HF calculations. Since we cannot impose a fixed-node boundary condition in these calculations our calculated $\partial_\lambda^n \Phi/\Phi$ may show a singular behaviour close to the nodes. Nevertheless, in our present applications to Zn_2,Cd_2, and Hg_2 we encountered no such difficulties,

but this might be different for other systems. Since this problem concerns only a small portion of the configuration space it should be possible to introduce some cut-off procedure for the higher-order terms near the nodes.

In our calculations of static dipole polarizabilities we have used the finite-difference approach in combination with the PDMC method of Caffarel and Claverie [37]. The energy is calculated via the time-dependent equation

$$E(\tau,\lambda) = \frac{\langle\Phi(0)\,|\,(\hat{H}_0+\hat{V}_\lambda)\,\exp\left[-(\hat{H}_0+\hat{V}_\lambda)\tau\right]\,|\,\Phi(0)\rangle}{\langle\Phi(0)\,|\,\exp\left[-(\hat{H}_0+\hat{V}_\lambda)\tau\right]\,|\,\Phi(0)\rangle}$$

$$= \lim_{T\to\infty} \frac{\int_0^T dt\,\frac{1}{2}\left(E_L(\lambda,\vec{r}_t)+E_L(\lambda,\vec{r}_{t+\tau})\right)\exp\left(-\int_t^{t+\tau}E_L(\lambda,\vec{r}_s)ds\right)}{\int_0^T dt\exp\left(-\int_t^{t+\tau}E_L(\lambda,\vec{r}_s)ds\right)}\ , \tag{16}$$

with the local energy

$$E_L(\lambda,\vec{r}) = \frac{\hat{H}_0\Phi(0)}{\Phi(0)} + \hat{V}_\lambda \tag{17}$$

and the field-dependent local potential

$$\hat{V}_\lambda = \partial_\lambda \frac{V_{pp}\Phi(\lambda)}{\Phi(\lambda)}\Big|_{\lambda=0}\lambda + \frac{1}{2}\partial_\lambda^2\frac{V_{pp}\Phi(\lambda)}{\Phi(\lambda)}\Big|_{\lambda=0}\lambda^2 + \sum_i z_i\lambda + V_{CPP}(\lambda)\ , \tag{18}$$

for an electric field parallel to the z axes. The right-hand side of Eq. (16) represents a fraction of path integrals extending over all paths of length τ which are generated by the stochastic differential equation

$$d\vec{x} = \frac{\nabla\Phi(0)}{\Phi(0)}dt + d\vec{W} \tag{19}$$

where $\vec{W}$ is a Wiener process. Since the trial wavefunction does not depend on the electric field the random walk is the same for different values of λ. This is equivalent to Wells approach [28] but involves no branching at all. The efficiency of the PDMC method compared to algorithms involving a branching step has been discussed elsewhere [38]. In the limit $\tau\to\infty$ we get the "exact" ground-state energy for the Schrödinger equation. From a single PDMC calculation one can obtain $E(\tau,\lambda)$ for different values of τ,λ without significantly increasing the computational effort compared to a single ground-state energy calculation. For a fixed value of τ we computed the static dipole polarizability $\alpha_D(\tau)$ by numerical differentiation, according to

$$\alpha_D(\tau) = \frac{2[E(\tau,2\lambda)+E(\tau,-2\lambda)] - 32[E(\tau,\lambda)+E(\tau,-\lambda)] + 60E(\tau,0)}{24\lambda^2} \tag{20}$$

From this data we took the limit $\alpha_D = \lim_{\tau\to\infty}\alpha_D(\tau)$. The convergence with respect to τ is plotted in Fig. 1. We tried $\lambda = 0.01, 0.001$ and obtained perfect agreement within the statistical uncertainties. We want to mention that the expansion of the localized pseudopotential is crucial to obtain a reasonable result. For the Hg atom we got, e.g. $\alpha_D = 31.9 \pm 0.4$ a.u. including only the linear term which differs by 4 a.u. from the α_D including the second-order term.

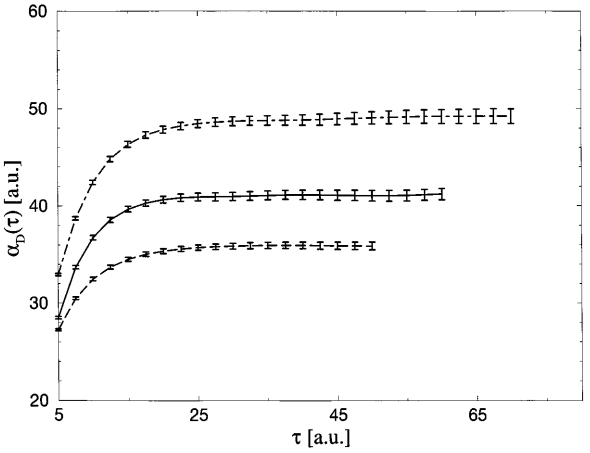

Fig. 1. Convergence of the dipole polarizabilities $\alpha_D(\tau)$ for Zn (*solid line*), Cd (*dashed-dotted line*) and Hg (*dashed line*) with respect to τ

2.4 Spectroscopic constants

The CCSD(T) spectroscopic constants were derived by fitting a fifth-degree polynomial in R times a factor 1/R for six calculated points on the potential curve near the equilibrium distance. A spacing of 0.1 a.u. between the points was used. The estimated numerical accuracy of the molecular constants is 0.01 eV, 0.01 Å and 1 cm^{-1}.

Due to the statistical uncertainties of the calculated energies at individual points of the potential curve a somewhat different approach had to be used for PDMC. To get reasonable estimates for the spectroscopic constants we supposed a simple Born-Mayer-type ansatz[39] for the potential curve

$$V_{BM} = -\frac{C}{R^6} + \beta\exp(-\alpha R)\ , \tag{21}$$

where the three independent parameters are optimized by a least-squares fit for a given set of energies at different interatomic distances. Since all the PDMC energies along the potential curve are statistically independent, it is possible to sample energies used in the least-squares fit and to obtain an estimate for the statistical error of the parameters. In each point we have sampled an energy from a Gaussian distribution with mean value and variance taken from the corresponding PDMC calculation. In order to check the reliability of the variance we have performed a Kolmogorov-Smirnov test [40] with our PDMC data see to see whether the variance is determined from a Gaussian distribution of statistically independent energies. This requirement was satisfied with good accuracy in all of our PDMC calculations. For these energies we have optimized the parameters of the potential and determined the spectroscopic constants. Repeating this procedure we obtained statistically independent sets of spectroscopic constants whose fluctuations represent the statistical uncertainties of the underlying PDMC energies.

2.5 Analysis of charge fluctuations

The bonding analysis has been performed on the basis of occupation number operators $\hat{N}$ defined in position space. Consider the homonuclear diatomic molecule to be aligned along the z-axis with the centre of mass in the origin. The space is then partitioned between both atoms by the plane $z = 0$ and the occupation operator for the atom located on the positive z-axis can be defined as

$$\hat{N} = \sum_{i=1}^{n} \Theta(z_i) \tag{22}$$

using the Heaviside's step function $\Theta(z_i)$. Its square is given by

$$\hat{N}^2 = \hat{N} + \sum_{i \neq j}^{n} \Theta(z_i)\Theta(z_j) \ . \tag{23}$$

Obviously for the systems considered here the average valence occupation $< \hat{N} >= 2$, independent of the wavefunction, and $< \hat{N}^2 >$ can be obtained using the fully generalized Feynman-Kac formula of Caffarel and Claverie [37]:

$$\frac{\langle \Phi \,|\exp\,(-\hat{H}\,\tfrac{\tau}{2})\,\hat{N}^2\exp(-\hat{H}\,\tfrac{\tau}{2})\,|\,\Phi\rangle}{\langle \Phi|\exp(-\hat{H}\tau)|\,\Phi\rangle} = \lim_{T\to\infty} \frac{\int_0^T dt \hat{N}^2(\vec{r}_{t+\frac{\tau}{2}}) \exp\left(-\int_t^{t+\tau} E_L(\vec{r}_s)ds\right)}{\int_0^T dt \exp\left(-\int_t^{t+\tau} E_L(\vec{r}_s)ds\right)} \ . \tag{24}$$

For $\tau = 0$ we obtain the expectation value for the trial wavefunction Φ. In the limit $\tau \to \infty$ it converges to the expectation value of the "exact" ground-state wavefunction. As discussed above the term "exact" has always to be understood within the fixed-node approximation. The charge fluctuation δN is given by

$$\delta N^2 = \langle \hat{N}^2 \rangle - \langle \hat{N} \rangle^2 \ . \tag{25}$$

The peculiar feature of this method is that the charge fluctuations can be calculated for arbitrary wavefunctions including the "exact" fixed-node wavefunction which gives a correct description of the bonding in these weakly bound molecules.

For heteronuclear diatomics, polyatomic clusters or molecules as well as solids the partitioning into atomic domains is less straightforward than for homonuclear diatomics. The use of Bader's zero-flux surfaces [41] appears to be a reasonable choice here.

3. Results and discussion

3.1 Atoms

The dispersion interaction for homonuclear dimers can be calculated with an approximation to London's formula, i.e.

$$\Delta E^{disp} = -3IP_1\alpha_D^2/(4R^6). \tag{26}$$

It is clear that any computational approach aiming at accurately calculating ΔE^{disp} has to yield good results for the first ionization potential (IP_1) and the dipole polarizability α_D of the neutral atom. The corresponding CCSD and PDMC values are summarized in Tables 3 and 4. At the self-consistent field (SCF) level the largest error in the IP is 0.04 eV (Hg) and in the dipole polarizability 2.6 a.u. (Hg). Since these errors are largest for the heaviest element of the group we mainly attribute them to frozen-core errors. The inclusion of core-valence correlation (CPP) and valence correlation (CCSD) increases IP_1 by about 1.5 eV. The theoretical values are still about $0.2 - 0.3$ eV smaller than the experimental results. The PDMC results are in excellent agreement with the CCSD values with a maximum deviation of 0.03 eV. Significantly better agreement between theory and experiment was obtained for small-core pseudopotentials [15]. However, such an approach is currently infeasible for the QMC study of the homonuclear dimers.

Dynamic and static polarization of the M^{2+} cores (CPP) leads to a reduction of the dipole polarizability α_D by up to 30% , whereas the inclusion of valence correlation (CCSD) has only minor effects. The calculated values are about $1.5 - 3.0$ a.u. too large compared to previous theoretical results using a small-core pseudopotential [15]. The PDMC results agree within the statistical errors with the CCSD values. A possible explanation for the discrepancies between small- and large-core pseudopotential calculations is the neglect of correlation effects on the core polarizabilities used in Eq. (3). We have tried to take this into account by using core polarizabilities obtained from finite-field CCSD(T) calculations with relativistic small-core pseudopotentials.

Table 3. First and second ionization potentials (IP_i) ($i = 1, 2$) (eV). AE (all-electron), DHF (Dirac-Hartree-Fock, PP (pseudopotential), SCF self-consistent field, CPP (core-polarization potential), CCSD coupled-cluster including single and double excitation operators, CCSD(T) coupled-cluster including single and double excitations, and triple excitations by perturbation theory, PDMC pure diffusion Monte Carlo

Method	Zn		Cd		Hg	
	IP_1	IP_2	IP_1	IP_2	IP_1	IP_2
AE; DHF	7.79	16.85	7.35	15.56	8.55	17.15
PP; SCF	7.77	16.86	7.34	15.56	8.51	17.10
PP, CPP; SCF	8.42	17.82	8.26	16.85	9.74	18.66
PP, CPP; CCSD	9.09	–	8.78	–	10.13	–
PP; CCSD(T)[a]	9.37	17.93	8.97	16.87	10.37	18.68
PP, CPP; PDMC[b]	9.11	–	8.81	–	10.16	–
Exp.[c]	9.39	17.96	8.99	16.91	10.44	18.75

[a] Small-core pseudopotential Ref. [15]
[b] Statistical errors are smaller than the last given digit
[c] Ref. [42]

Table 4. Dipole polarizabilities α_D (a.u.)

Method	Zn	Cd	Hg
AE; DHF	50.8	63.7	44.8
PP; SCF	51.4	65.2	47.4
PP, CPP; SCF	41.8	48.4	34.8
PP; CCSD(T)[a]	38.3	46.0	34.2
PP, CPP; CCSD	41.5	49.2	35.7
PP, CPP; CCSD[c]	40.6	48.7	35.2
PP, CPP; PDMC	41.1 ± 0.5	49.2 ± 0.7	35.9 ± 0.3
Exp.[b]	38.8 ± 0.8	49.7 ± 1.6	33.9 ± 0.3

[a] Small-core pseudopotential Ref. [15]
[b] Refs. [43–45]
[c] CPP with α_D from correlated calculations

The results listed in Table 4 show only minor improvements. The remaining discrepancies cannot be explained in such a simple manner and indicate principal limitations of the CPP method for large-core pseudopotentials.

A slight systematic underestimation of IP_1 and overestimation of α_D yields too large absolute values of London's dispersion energy. The errors are of the order of 14% for Zn, 12% for Cd and 6% for Hg. Despite of these inaccuracies the large-core pseudopotentials appear to be sufficiently accurate to be applied to the study of the weak-bonding interaction in the group 12 dimers.

3.2 The Zn_2, Cd_2 and Hg_2 molecules

The results for bond lengths, binding energies and vibrational constants of Zn_2 and Cd_2 are listed in Table 5. Corresponding results for Hg_2 [10, 11] are also included. The experimental binding energy of the group 12 dimers increases from Zn_2 to Hg_2, whereas the vibrational frequency decreases at the same time. No experimental data for the bond lengths of Zn_2 and Cd_2 are available to our knowledge, however, previous small-core pseudopotential calculations indicate that the bond lengths of Zn_2 and Cd_2 are very similar and about 0.2 Å larger than for Hg_2. The present large-core pseudopotential CCSD(T) calculations reproduce well the experimental increase of the binding energy from Zn_2 to Hg_2. The largest deviation from experimental values occurs for Zn_2 (0.012 eV), however, the error with respect to a previous result [15] obtained with a small-core pseudopotential is much smaller. The present work predicts the bond length of Cd_2 to be about 0.12 Å and 0.46 Å longer than for Zn_2 and Hg_2, respectively. The derived vibrational frequencies agree with those from previous small-core pseudopotential calculations within 2 cm^{-1} or less.

Let us now turn to the QMC results for Zn_2 and Cd_2. The PDMC and CCSD(T) energies are in good agreement for all points of the potential curve (Fig. 2). The derived spectroscopic constants listed in Table 5 are in reasonable correspondence with the CCSD(T) values. Binding energies are close to the CCSD(T) results, whereas the vibrational constants are slightly too large. The most striking differences are the shorter PDMC bond lengths but in view of the flat shape of the potential-energy curves this should not be overrated.

As already mentioned for the atoms, dipole polarizabilities play an important role for the interaction of van der Waals clusters. We have therefore performed some test calculations for the molecules Zn_2, Cd_2 and Hg_2 for which we have determined the tensor component of the dipole polarizability parallel to the molecular axis. The results listed in Table 5 show that the relative errors of the large-core compared to the small-core pseudopotentials are of the same order of magnitude for atoms and molecules. The PDMC results again agree very well with those from CCSD(T) calculations.

3.3 The Be_2 molecule

The molecules Zn_2, Cd_2 and Hg_2 are well described within the fixed-node approximation by a single-reference trial wavefunction. A more serious challenge for the fixed-node approximation is the Be_2 molecule which is well-known for the difficulties it provides in standard ab initio calculations due to the near-degeneracy of the $2s$ and $2p$ atomic orbitals. In order to get a trial wavefunction for the Be atom which provides a reasonable description of the nodal structure it is necessary to include at least the $2s^2$ and $2p^2$ configurations [46]. This is equivalent to performing a complete-active-space self-

Table 5. Bond lengths R_e (Å), binding energies D_e (eV), vibrational constants ω_e (cm^{-1}) and dipole polarizabilities α_D (a. u.) along the molecular axes for Zn_2, Cd_2 and Hg_2

	Method	Zn_2	Cd_2	Hg_2[a]
R_e	PP, CPP; CCSD(T)	4.11	4.23	3.77
	PP, CPP; PDMC	3.88 ± 0.05	4.05 ± 0.03	3.74 ± 0.04
	PP; CCSD(T)[b]	3.96	3.96	3.77
	Exp.[c]			3.63 ± 0.04
D_e	PP, CPP; CCSD(T)	0.022	0.029	0.044
	PP, CPP; PDMC	0.024 ± 0.007	0.031 ± 0.005	0.056 ± 0.007
	PP; CCSD(T)[b]	0.024	0.036	0.044
	Exp.[c]	0.034	0.039	0.043 ± 0.003
ω_e	PP, CPP; CCSD(T)	21	18	19
	PP, CPP; PDMC	25 ± 2	21 ± 1	22 ± 1
	PP; CCSD(T)[b]	22	20	19
	Exp.[c]	25.7 ± 0.2	22.5 ± 0.2	18.5 ± 0.5
α_D	PP, CPP; CCSD(T)	102.3	124.8	92.4
	PP, CPP; PDMC	102.7 ± 1.1	125.4 ± 2.1	91.7 ± 0.7
	PP; CCSD(T)[d]	95.6	122.1	87.4

[a] Ref. [11]
[b] Small-core pseudopotential Ref. [15]
[c] Ref. [1–3]
[d] Small-core pseudopotential

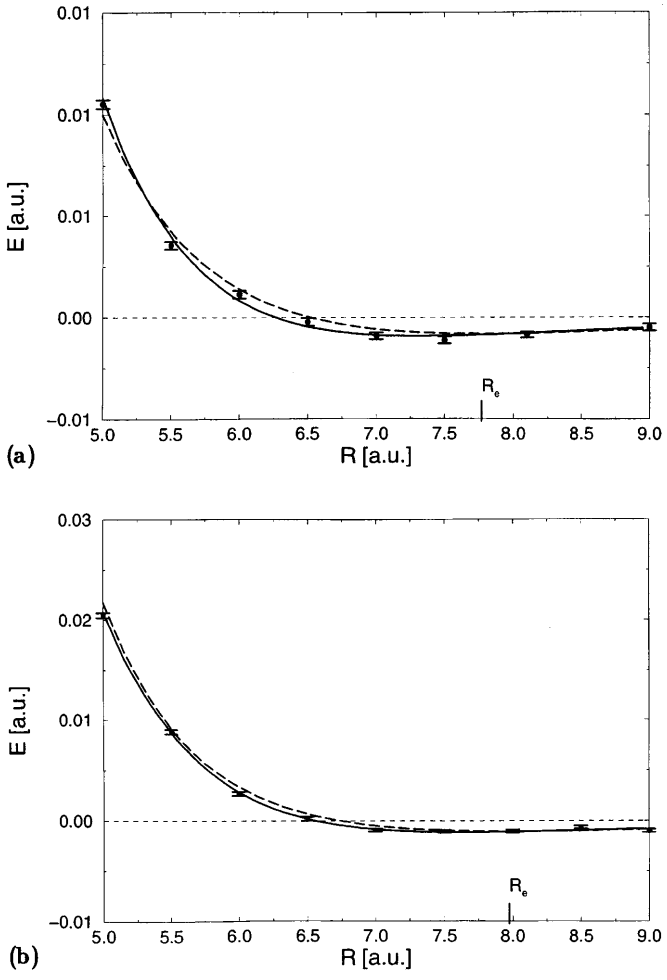

Fig. 2a,b. Potential curves for: **a** Zn_2 and **b** Cd_2 from PP, CPP CCSD(T) (*dashed line*) and PDMC (*solid line*) calculations. The indicated equilibrium distance relates to the CCSD (T) curve

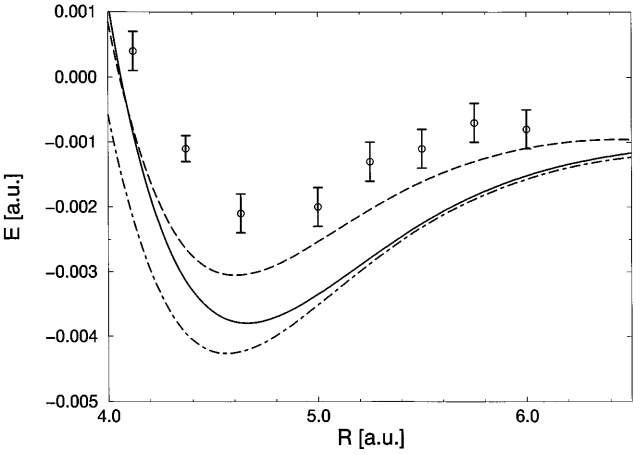

Fig. 3. Potential curves for Be_2 from PDMC and other ab initio methods. Single point PDMC results ○ are given with error bars. Extended geminal model of Røeggen and Almlöf [47] (*solid line*), multi-reference PP, CPP, ACPF calculations (*dashed-dotted line*), PP, CPP, CCSD(T) calculations (*dashed line*).

consistent field (CASSCF) calculation in the valence space. With such a trial wavefunction one obtains 99.1% of the atomic correlation energy in all-electron calculations. For the Be_2 molecule we did not include the full CAS spanned by two σ_g, two σ_u, one π_u and one π_g orbitals but rather restricted ourselves to the subset of configurations which contribute in the limit of infinite separation. At the equilibrium distance such a MCSCF wavefunction recovers 98.5% of the CASSCF correlation energy. Our trial wavefunction includes all closed-shell CSFs and those arising from the $2\sigma_g^1 2\sigma_u^1 1\pi_u^1 1\pi_g^1, 2\sigma_g^1 3\sigma_g^1 2\sigma_u^1 3\sigma_u^1, 1\pi_u^2 1\pi_g^2$ and $3\sigma_g^1 3\sigma_u^1 1\pi_u^1 1\pi_g^1$ configurations with all orbitals at most singly occupied. In Fig. 3 we have plotted the potential-energy curves obtained from PDMC, CCSD(T) and averaged coupled-pair functional (ACPF) calculations. The deepest potential well has been obtained from ACPF calculations and is even lower than that found by Røeggen and Almlöf [47]. The agreement between both curves is good for distances larger than 5 bohr and becomes worse in the inner region. The PP + CPP approach seems to overestimate the attractive interactions, leading to a shorter bond distance of 4.56 bohr compared to 4.67 bohr [47] and 4.627 bohr [19] obtained from all-electron calculations. The CCSD(T) curve has a similar shape but is significantly shallower indicating the need for a multi-reference ansatz for the wavefunction. In our PDMC calculations we obtained a reasonable shape but again the potential-energy curve is much too shallow. Although we have used the same reference space as in our ACPF calculation there still seems to be a fixed-node error left. This is not really surprising since previous studies using MCSCF trial wavefunctions [33, 48] have shown that taking into account near-degeneracies often removes only a part of the fixed-node error. Dynamic correlation may also have some effects on the nodal structure but a reasonable ansatz for taking it into account in the trial wavefunction is still missing. Nevertheless we got a bonding interaction which cannot be obtained from HF nodes where the total energy at the equilibrium distance is 13.6 millihartree (mH) higher. To confirm our finding we have performed a single all-electron PDMC calculation at R = 4.63 bohr using the same type of MCSCF trial wavefunction. We obtained a total energy of -29.3350 ± 0.0006 H which is lower than that obtained by Filippi and Umrigar [48] (-29.3301 ± 0.0002)H with a trial wavefunction including the configurations $2\sigma_g^2 2\sigma_u^2, 2\sigma_g^2 3\sigma_g^2, 2\sigma_g^2 1\pi_u^2$ and $2\sigma_g^1 2\sigma_u^1 1\pi_u^1 1\pi_g^1$. The binding energy of 1.9 ± 1.2 mH is not very meaningful due the relatively large statistical error but it clearly indicates that all-electron and pseudopotential calculations are in good agreement.

3.4 Charge fluctuations

Finally we want to discuss the atomic charge fluctuations of Zn_2, Cd_2, Hg_2 and Be_2. Previous work by Mödl et al. [18] and Yu and Dolg [15] used occupation number operators defined by means of localized orbitals. Since a pure van der Waals interaction results from simultaneous intraatomic excitations (e.g. $s^2 \rightarrow s^1 p^1$ on both atoms) no charge fluctuations were observed, e.g. for

He_2 at the equilibrium distance. The presence of charge fluctuations within this definition is only possible at the correlated level and indicates covalent bonding. For Zn_2, Cd_2 and Hg_2 roughly $25-30\%$ of the covalent bonding contribution was estimated [15]. The present position space definition of the occupation-number operator yields quite different results. For the SCF wavefunction in a basis of localized orbitals one finds non-zero charge fluctuations since the exponential tail of an orbital localized on one atom reaches into part of the space associated with the other atom. This means that the assignment of localized orbitals to atoms can be done only in an approximate way. It can be easily seen that $\delta N^2 \alpha \langle \Theta(z)\phi | \Theta(z)\phi \rangle$ where ϕ is the orbital with its centre on the negative z-axis. Due to the exponential decay of the orbitals the logarithm of the charge fluctuation is a linear function of the bond distance as can be seen in Fig. 4. Electron correlation, accounted for at the PDMC level, virtually does not change the picture. The stronger the covalent contribution to bonding, the less the electrons are equally distributed between the two atomic domains, i.e. an increase of the charge fluctuations is observed. The relative magnitude of the covalent-bonding contributions at equilibrium distance estimated from $\sqrt{< \delta N^2 >}$ is very similar for the present and previous definitions of the occupation-number operator ($Zn_2 < Cd_2 \simeq Hg_2$).

Of special interest is a comparison with Be_2, a system which is well-known for large covalent bonding contributions [19]. The charge fluctuations are significantly larger than for the group 12 dimers. Electron correlation has a noticeable influence and we can distinguish between static and dynamic correlation. For the HF wavefunction we obtained a nearly linear decrease on a logarithmic scale for the same reasons already discussed above. The Variational Monte Carlo (VMC) results refer to expectation values of our trial wavefunction which includes all the static correlation effects. There is also some dynamic correlation included due to the correlation factor F, but in this special case F is only of minor importance as can be seen from its small contributions to the correlation energy. Static correlation suppresses the charge fluctuations considerably with a similar linear decrease on a logarithmic scale as HF. If we include dynamic correlation by doing PDMC we get a slight increase in the charge fluctuations compared to VMC. There is a weak shoulder around 5.5 bohr which appears at a position where the localized orbital based approach starts to decrease linearly on a logarithmic scale.

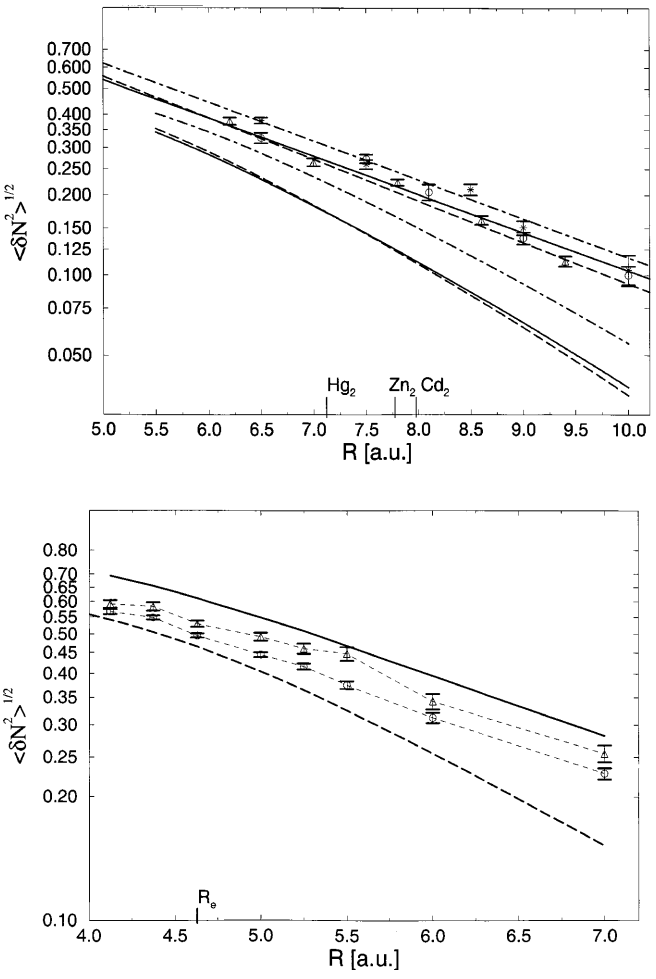

Fig. 4a,b. Interatomic charge fluctuations $\sqrt{\langle \delta N^2 \rangle}$ for: **a** Zn_2, Cd_2 and Hg_2. The upper three lines refer to HF results for Zn_2 (*solid line*), Cd_2 (*dashed-dotted line*) and Hg_2 (*dashed line*), obtained from Eq. (23) whereas the lower three lines are taken from Yu and Dolg [15]. The PDMC results are given with error bars for Zn_2, $\circ$, Cd_2 $*$, Hg_2 Δ. Equilibrium distances obtained from PP, CPP, CCSD (T) calculations are indicated: **b** Be_2, the PDMC Δ and VMC $\circ$ results are given with error bars. For comparison HF (*solid line*) and localized orbital based (*dashed line*) results are also indicated

4. Conclusions

PDMC techniques applied together with relativistic large-core pseudopotentials and core-polarization potentials are able to yield accurate molecular constants for very weakly interacting systems such as the group 12 homonuclear dimers Zn_2, Cd_2 and Hg_2. The approach is ideally suited for the study of larger clusters of these atoms, e.g. in order to investigate the transition from van der Waals to covalent and finally metallic bonding. The feasibility of PDMC calculations for static dipole polarizabilities using the finite-field approach has been demonstrated. Special emphasis has been given to the response of the localized pseudopotential to the external electric field. An analysis of the wavefunction in terms of charge fluctuations obtained for spatially defined operators shows covalent bonding contributions in the order $Zn_2 < Cd_2 \simeq Hg_2$ at the equilibrium distance. For comparisons we have studied the related Be_2 molecule. Our calculations demonstrate the applicability of QMC methods even in the case of strong near-degeneracies.

Acknowledgements. The authors are grateful to Prof. P. Fulde, Dresden, for continuous support.

References

1. van Zee RD, Blankespoor SC, Zwier TS (1988) J Chem Phys 88:4650

2. Czajkowski M, Bobkowski R, Krause L (1989) Phys Rev A 40:4338
3. Czajkowski M, Bobkowski R, Krause L (1990) Phys Rev A 41:277
4. Koperski J, Atkinson JB, Krause L (1994) Chem Phys Lett 219:161
5. Koperski J, Atkinson JB, Krause L (1994) Can J Phys 72:1070
6. Balasubramanian K, Das KK, Liao DW (1992) Chem Phys Lett 195:487
7. Schwerdtfeger P, Li J, Pyykkö P (1994) Theor Chim Acta 87:313
8. Czuchaj E, Rebentrost F, Stoll H, Preuss H (1994) Chem Phys Lett 225:233
9. Bierón JR, Baylis WE (1995) Chem Phys 197:129
10. Dolg M, Flad HJ (1996) J Phys Chem 100:6147
11. Flad HJ, Dolg M (1996) J Phys Chem 100:6152
12. Kunz CF, Hättig C, Heß BA (1996) Mol Phys 89:139
13. Czuchaj E, Rebentrost F, Stoll H, Preuss H (1996) Chem Phys Lett 255:203
14. Czuchaj E, Rebentrost F, Stoll H, Preuss H (1997) Chem Phys 214:277
15. Yu M, Dolg M (1997) Chem Phys Lett 273:329
16. Dolg M, Flad HJ (1997) Mol Phys 91:815
17. Anderson JB, Traynor CA, Boghosian BM (1993) J Chem Phys 99:345
18. Mödl M, Dolg M, Fulde P, Stoll H (1996) J Chem Phys 105:2353
19. Stärck J, Meyer W (1996) Chem Phys Lett 258:421
20. (a) Müller W, Flesch J, Meyer W (1984) J Chem Phys 80:3297; (b) Müller W, Meyer W (1984) J Chem Phys 80:3311
21. (a) Fuentealba P, Preuss H, Stoll H, v Szentpály L (1982) Chem Phys Lett 89:418; (b) v Szentpály L, Fuentealba P, Preuss H, Stoll H (1982) Chem Phys Lett 93:555
22. Küchle W, Dolg M, Stoll H, Preuß H (1991) Mol Phys 74:1245
23. MOLPRO is a package of ab initio programs written by Werner HJ, Knowles PJ, with contributions from Almlöf J, Amos RD, Deegan MJO, Elbert ST, Hampel C, Meyer W, Peterson K, Pitzer RM, Stone AJ, Taylor PR; Hampel C, Peterson K, Werner HJ (1992) Chem Phys Lett 190:1
24. Magnasco V, McWeeny R (1991) In: Maksić ZB (ed) Theoretical models of chemical bonding. vol 4. Springer, Berlin, p 113
25. Caffarel M, Hess O (1991) Phys Rev A 43:2139
26. Caffarel M, Hess O (1991) Advances in biomolecular simulations. American Institute of Physics Conference Proceedings No. 239:20
27. Caffarel M, Rérat M, Pouchan C (1993) Phys Rev A 47:3704
28. Wells BH (1985) Chem Phys Lett 115:89
29. Vrbik J, Legare DA, Rothstein SM (1990) J Chem Phys 92:1221
30. Huiszoon C, Briels WJ (1993) Chem Phys Lett 203:49
31. East ALL, Rothstein SM, Vrbik J (1988) J Chem Phys 89:4880; East ALL, Rothstein SM, Vrbik J (1990) 92:2120
32. Reynolds PJ (1990) J Chem Phys 92:2118
33. Flad HJ, Caffarel M, Savin A (1997) In: Lester WA Jr (ed) Recent advances in quantum Monte Carlo methods. World Scientific, Singapore, p 73
34. Fahy S, Wang XW, Louie SG (1990) Phys Rev B 42:3503
35. Mitáš L, Shirley EL, Ceperley DM (1991) J Chem Phys 95:3467
36. Hammond BL, Lester WA Jr, Reynolds PJ (1994) Monte Carlo methods in ab initio quantum chemistry. World Scientific, Singapore
37. Caffarel M, Claverie P (1988) J Chem Phys 88:1088; Caffarel M, Claverie P (1988) 88:1100
38. Flad HJ, Dolg M (1997) J Chem Phys 107:7951
39. Born M, Mayer JE (1932) Z Physik 75:1
40. Press WH, Flanery BP, Teukowsky SA, Vetterling WT (1986) Numerical recipes. Cambridge University Press, Cambridge
41. Bader RFW, Nguyen-Dang TT (1981) Adv Quantum Chem 14:63
42. Moore CE (1958) Atomic energy levels, Circ Nat Bur Stand 467. United States Department of Commerce, Washington D.C.
43. Göbel D, Hohm U, Maroulis G (1996) Phys Rev A 54:1973
44. Göbel D, Hohm U (1995) Phys Rev A 52:3691
45. Göbel D, Hohm U (1996) J Phys Chem 100:7710
46. Harrison RJ, Handy NC (1985) Chem Phys Lett 113:257
47. Røeggen I, Almlöf J (1996) Int J Quantum Chem 60:453
48. Filippi C, Umrigar CJ (1996) J Chem Phys 105:213